

Supporting Information File

Concomitant spin-canted antiferromagnetic ordering and proton conduction in homoleptic and homometallic coordination polymers

Soumyabrata Goswami, Soumava Biswas and Sanjit Konar*

*Department of Chemistry, IISER Bhopal, Indore By-pass Road, Bhauri, District: Bhopal – 462066,
Madhya Pradesh - India. Fax: +91-755-6692392; Tel: +91-755-6692339
E-mail: skonar@iiserb.ac.in*

1) EXPERIMENTAL SECTION

1a) Materials: All the reagents and solvents were commercially available and were used as obtained. Potassium salt of oxonic acid, $\text{Fe}(\text{ClO}_4)_2 \cdot 6\text{H}_2\text{O}$ and $\text{Co}(\text{ClO}_4)_2 \cdot 6\text{H}_2\text{O}$ were obtained from the Sigma Aldrich Chemical Co.

Caution! Perchlorate salts are potentially hazardous, so these salts should be used in minimum amounts and proper caution should be taken when dealing with such salts.

1b) Methods: The elemental analyses were carried out on Elementar Microvario Cube Elemental Analyzer. FT-IR spectra ($4000 - 500 \text{ cm}^{-1}$) were recorded on KBr pellets with a Perkin-Elmer Spectrum BX spectrometer. Powder X-ray diffraction (PXRD) data were collected on a PANalytical EMPYREAN instrument using Cu-K α radiation. Magnetic measurements were performed using a SQUID VSM magnetometer (Quantum Design). The measured values were corrected for the experimentally measured contribution of the sample holder, while the derived susceptibilities were corrected for the diamagnetism of the samples, estimated from Pascal's tables.¹ Adsorption studies were performed by using BELsorp Aqua3 (BEL Japan) volumetric solvent adsorption analyser. Water used was of Ultra-pure research grade (99.9%). Prior to the measurements a known weight of adsorbent powder sample was pre-treated for 12 h under 10^2 kPa continuous vacuum using BelPrepvacII at 100 °C. Proton conductivities were measured using the conventional quasi four-probe method on pellet sample (diameter of 13 mm and thickness of 0.5 and 0.8 mm respectively for Fe and Co complexes) using two gold electrodes attached to the surface. The AC impedance measurements were carried out with Solartron SI 1260 impedance analyzer under controlled temperature and humidity conditions.

1c) Synthesis of $\{[\text{Fe}_3(\text{L})_3(\text{H}_2\text{O})_6]_n \cdot 13n(\text{H}_2\text{O})\}$ (1):

Potassium oxonate (0.5 mmol, 98 mg) was taken in 15 mL of water and stirred for 20 min to dissolve. $\text{Fe}(\text{ClO}_4)_2 \cdot \text{H}_2\text{O}$ (0.5 mmol, 127 mg) was dissolved in 15 mL of methanol, and 3 mL of this Fe(II) solution was slowly and carefully layered over 3 mL of the ligand solution, using 2 mL of a 1:1 mixture of water and methanol as a third middle layer to slow down the diffusion, in a narrow glass tube. Brown colored block-shaped crystals were formed after one week in the tube. The crystals were separated, washed with cold water and Et_2O , and air dried (yield 78%). Anal. Calcd for $\text{C}_{24}\text{H}_{56}\text{Fe}_6\text{N}_{18}\text{O}_{49}$: C, 16.80; H, 3.29; N, 14.69 %. Found: C, 16.59; H, 3.50; N, 14.51 %. FT-IR (KBr pellet, $4000 - 500 \text{ cm}^{-1}$): $\nu(\text{O}-\text{H})$ 3448 cm^{-1} and $\nu(\text{O}=\text{C}-\text{N}-\text{H})$ 1641 cm^{-1} (Fig. S8).

1d) Synthesis of $\{[\text{Co}_3(\text{L})_3(\text{H}_2\text{O})_6]_n \cdot 13n(\text{H}_2\text{O})\}$ (2):

Complex **2** was synthesised in a manner similar to **1** except $\text{Co}(\text{ClO}_4)_2 \cdot 6\text{H}_2\text{O}$ (0.5 mmol, 183 mg) was used instead of $\text{Fe}(\text{ClO}_4)_2 \cdot \text{H}_2\text{O}$. Pink block-shaped crystals were formed after one week in the tube. The crystals were separated, washed with cold water and Et_2O , and air dried (yield 80%). Anal. Calcd for $\text{C}_{24}\text{H}_{56}\text{Co}_6\text{N}_{18}\text{O}_{49}$: C, 16.62; H, 3.25; N, 14.54 %. Found: C, 16.21; H, 3.31; N, 14.20 %. FT-IR (KBr pellet, $4000 - 500 \text{ cm}^{-1}$): $\nu(\text{O}-\text{H})$ 3439 cm^{-1} and $\nu(\text{O}=\text{C}-\text{N}-\text{H})$ 1650 cm^{-1} (Fig. S8).

2) Single Crystal Data Collection and Structure Determination:

Single crystal X-ray data collection of the complexes were performed at 307 K on a Bruker Smart Apex-II CCD diffractometer with graphite monochromated Mo-K α ($\lambda = 0.71073 \text{ \AA}$) radiation. Data collections were performed using ϕ and ω scans. The structures were solved using direct methods followed by full matrix least-squares refinements against F^2 (all data HKLF 4 format) using SHELXTL.² A multiscan absorption correction, based on equivalent reflections, was applied to the data. Anisotropic refinement was used for all non-hydrogen atoms except disordered solvent molecule. Whenever possible, the hydrogen atoms were located on a difference Fourier map and refined. In other cases, the hydrogen atoms were geometrically fixed. Crystallographic data are summarized in table S2 in Supporting Information and CIF files for the structures reported in this paper have been deposited with the Cambridge Crystallographic Data Centre (CCDC). CCDC-1014970 (complex **1**) and 1014971 (complex **2**), contain the supplementary crystallographic data for the paper. Copies of the data can be obtained, free of charge on application to the CCDC, 12 Union Road, Cambridge, CB2 1EZ UK [Fax: 44 (1233) 336 033 e-mail: deposit@ccdc.cam.ac.uk].

Table S1. Comparison of Proton Conductivity of some magnetic MOFs or coordination polymers at specified condition.

Complexes	Proton Conductivity [S cm^{-1}]	Temperature (K)	Humidity [RH%]	Ref. in main text
Co[Cr(CN) ₆] _{2/3} ·zH ₂ O	1.7x10 ⁻³	308	100	8d
V[Cr(CN) ₆] _{2/3} ·zH ₂ O	2.6x10 ⁻³	323	100	8d
(NH ₄) ₄ [MnCr ₂ (ox) ₆] ₃ ·4H ₂ O	1.7x10 ⁻³	313	96	8c
{NEt ₃ (CH ₂ COOH)}[MnCr(ox) ₃]	1x10 ⁻⁷	298	65	8b
{NH(prol) ₃ } [MCr(ox) ₃] (M = Mn ^{II} , Fe ^{II} , Co ^{II})	1x10 ⁻⁴	298	75	8a
[H ₃ O] ₂ [Mn ₇ (μ ₃ OH) ₄ (C ₁₄ H ₈ O ₆ S) ₆ (H ₂ O) ₄] (H ₂ O) ₂ (DMF) ₈	3.44x10 ⁻⁴	308	98	8e
{[M ₃ (HL) ₃ (H ₂ O) ₆] _n ·13n(H ₂ O)} [M = Fe (1), Co (2)]	1.3 x 10 ⁻⁶ (1) 1.2 x 10 ⁻⁴ (2)	353	95	Our work

Table S2. X-Ray Crystallographic Data and Refinement Parameters for **1** and **2**.

	1	2
Formula	C ₂₄ H ₅₆ Fe ₆ N ₁₈ O ₄₉	C ₂₄ H ₅₆ Co ₆ N ₁₈ O ₄₉
M _w (g mol ⁻¹)	1715.86	1734.39
Crystal size (mm)	0.40×0.33×0.29	0.42×0.35×0.29
Crystal system	Tetragonal	Tetragonal
Space group	P4 ₂ /n	P4 ₂ /n
T (K)	307	307
a (Å)	14.300(4)	14.204(9)
b (Å)	14.300(4)	14.204(9)
c (Å)	14.983(4)	15.037(10)
α(°)	90.00	90.00
β(°)	90.00	90.00
γ(°)	90.00	90.00
V (Å ³)	3063.9(19)	3033.8(4)
Z	2	2
ρ _{calcd} (g cm ⁻³)	1.832	1.870
μ(MoKα) (mm ⁻¹)	1.513	1.734
F(000)	1696.0	1708.0
T _{max} , T _{min}	0.645, 0.555	0.605, 0.488
h, k, l range	-17 ≤ h ≤ 17, -17 ≤ k ≤ 17, -17 ≤ l ≤ 17	-19 ≤ h ≤ 19, -19 ≤ k ≤ 19, -20 ≤ l ≤ 20
Collected reflections	2690	4288
Independent reflections	2136	2477
Goodness-of-fit (GOF) on F ²	1.018	0.981
R1, wR2 (I > 2σI) ^a	0.0512, 0.1456	0.0567, 0.1642
R1, wR2 (all data) ^a	0.0640, 0.1547	0.1068, 0.1913
CCDC Number	1014970	1014971

^a R₁ = $\sum|F_o| - |F_c|/\sum|F_o|$ and wR₂ = $[\sum w(|F_o|^2 - |F_c|^2)]/[\sum w(F_o)^2]^{1/2}$.

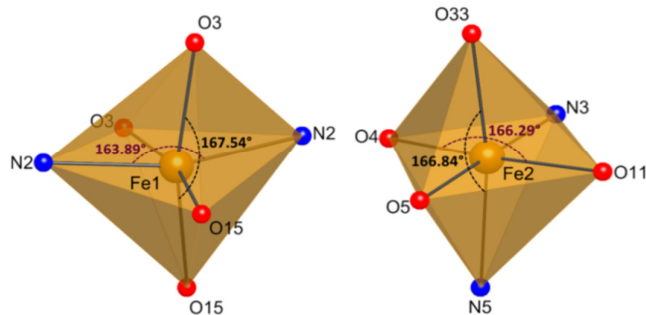


Fig. S1. Polyhedral view of the coordination environment around the two crystallographically independent Fe^{II} centers found in **1**.

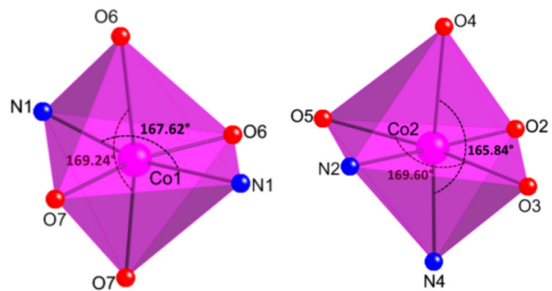


Fig. S2. Polyhedral view of the coordination environment around the two crystallographically independent Co^{II} centers found in **1**.

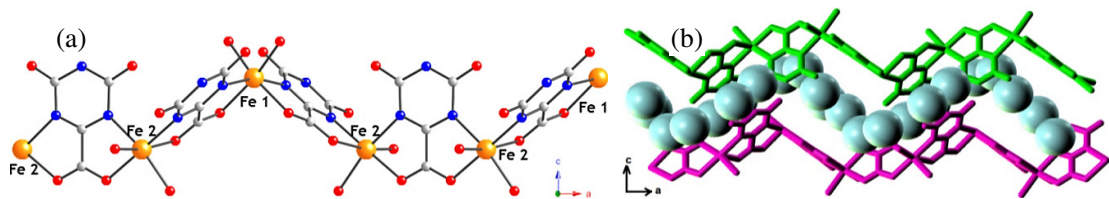
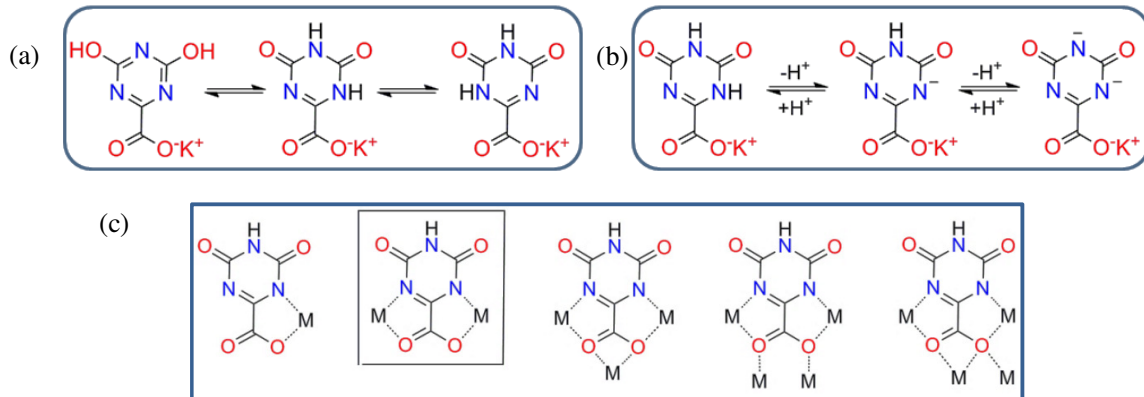


Fig S3. (a) View of a portion of the 1D zig-zag chain for **1**. Color codes: Saffron-Fe, red-O, blue-N and light gray-C. Hydrogen atoms are omitted for clarity; (b) Illustration of the continuous water channel between two adjacent 1D chains (shown by green and pink colors for clarity) for the complexes.



Scheme S1. (a) Illustration of reorganisation of the π bond and intramolecular H⁺ transfer between the tautomers in KH₂oxonate. (b) KH₂oxonate, with all its deprotonated forms possible. (c) Bridging modes of the oxonate ligand with metal centers. The encircled one represents the bridging mode in the reported complexes.

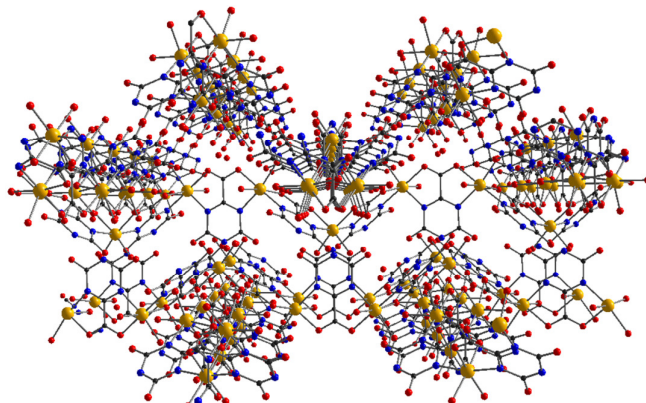


Fig. S4. Packing diagram of complex **1** viewed along *a*-axis.

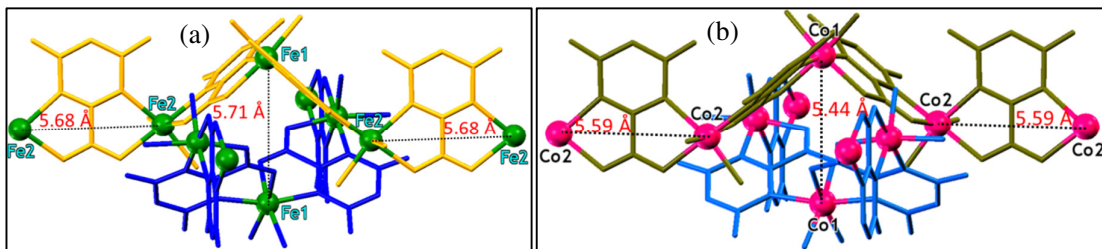


Fig. S5 Intra-chain and inter-chain M···M bond distances in (a) complex 1; (b) complex 2.

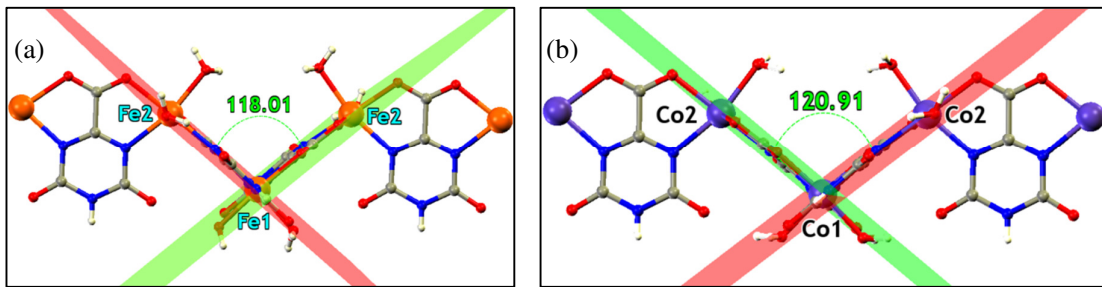


Fig. S6. Dihedral angle between two adjacent planes containing the metal centers in (a) complex 1; (b) complex 2.

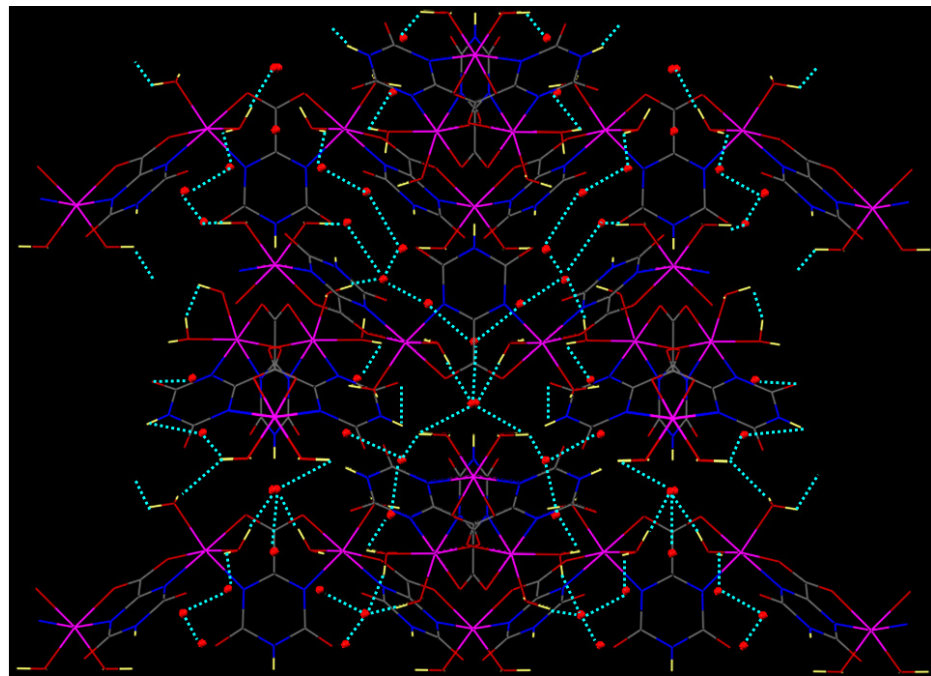


Fig. S7. Illustration of intra- and inter-chain H-bonding interactions involving coordinated and non-coordinated H₂O molecules, the triazine NH moieties, and the exocyclic oxygen atoms to form a 3D supramolecular network.

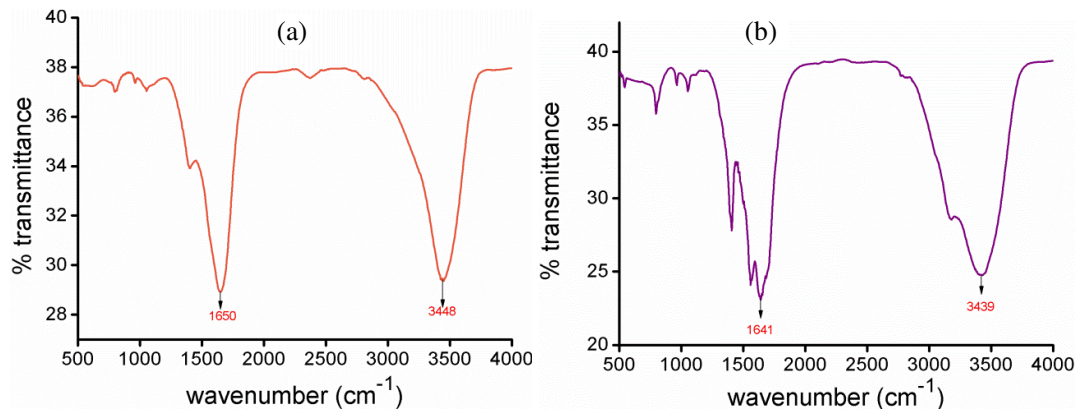


Fig. S8. FT-IR spectra for (a) complex **1** and (b) complex **2**.

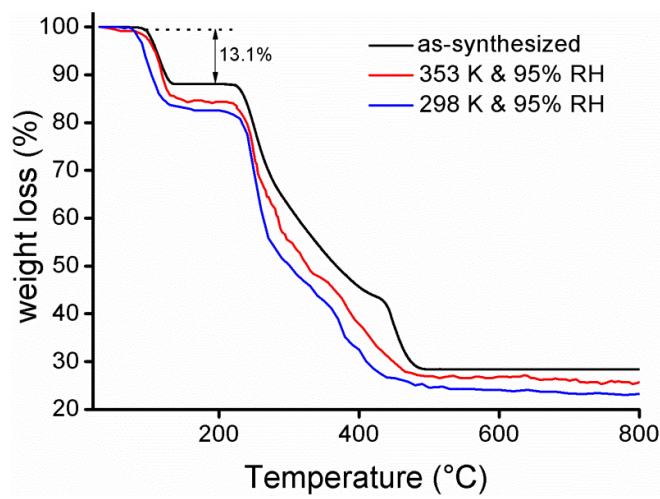


Fig. S9. Thermogravimetric analysis data for complex **1**.

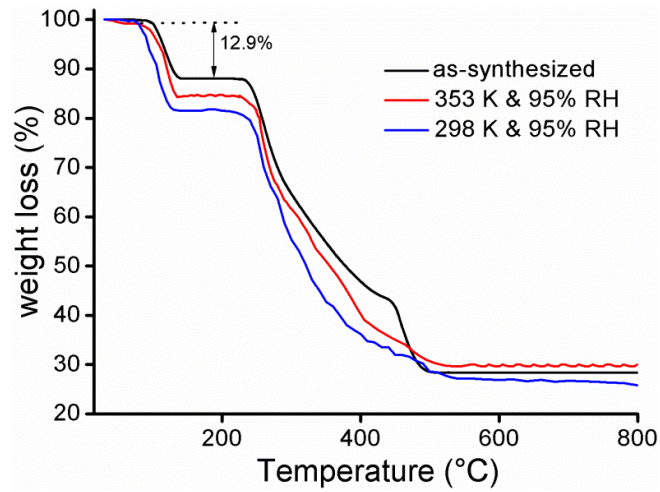


Fig. S10. Thermogravimetric analysis data for complex **2**.

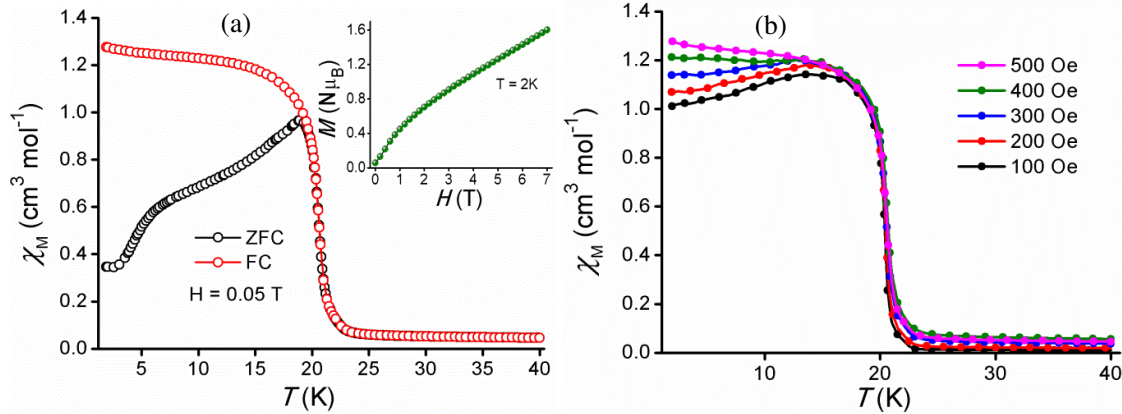


Fig. S11 (a) χ_M vs. T plot measured at 0.05 T showing bifurcation of FC and ZFC curves below 19 K ; Inset: Field dependence of magnetization of **1** at 1.8 K ; (b) Temperature dependence of the field-cooled magnetization (FCM) at various fields.

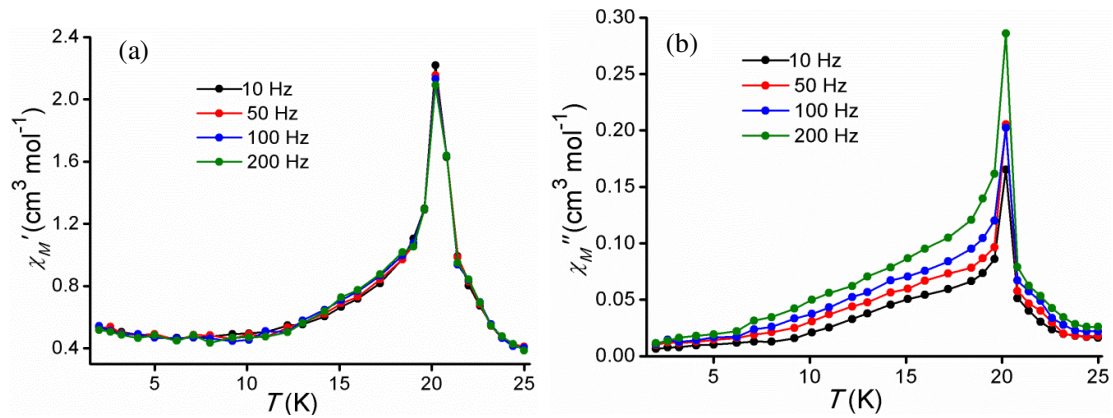


Fig. S12. In-phase (a) and out-of-phase (b) AC magnetic susceptibility plots for complex **1**.

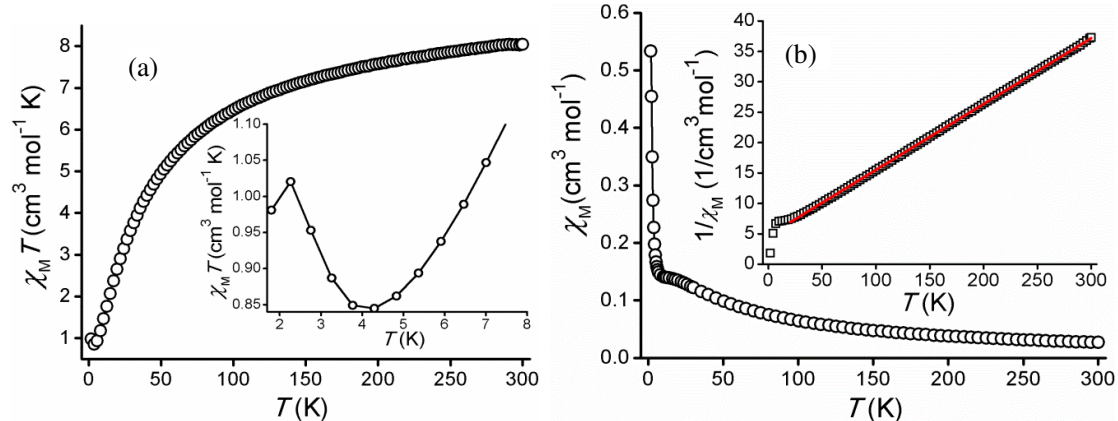


Fig. S13. (a) Temperature dependence of $\chi_M T$ measured at 0.1 T for complex **2**. Inset curve shows magnification of the low temperature region; (b) χ_M vs. T measured at 0.1 T . Inset graph shows inverse susceptibility curve and its Curie-Weiss fitting (red line).

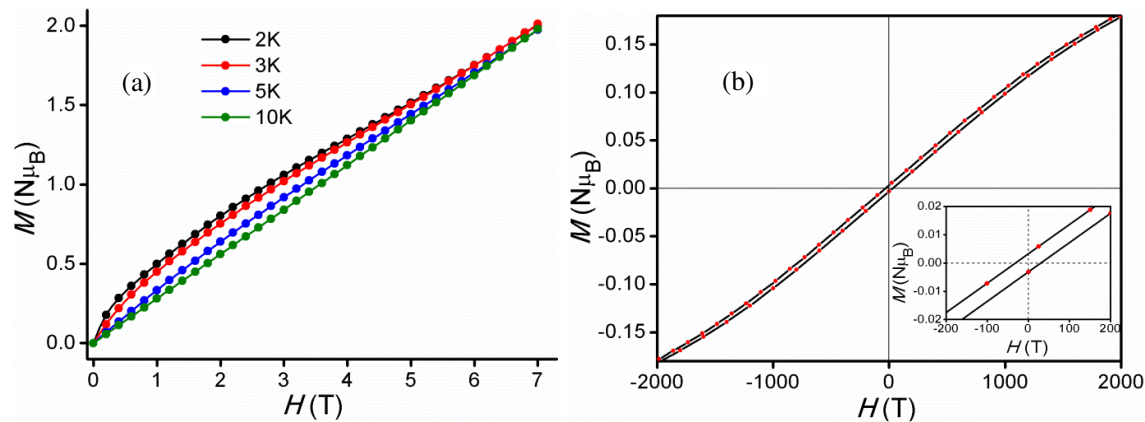


Fig. S14. (a) Isothermal magnetization curves for **2** at 2, 3, 5 and 10 K; (b) Hysteresis loop for **2** measured at 1.8 K. Inset graph shows broadened region of the hysteresis plot.

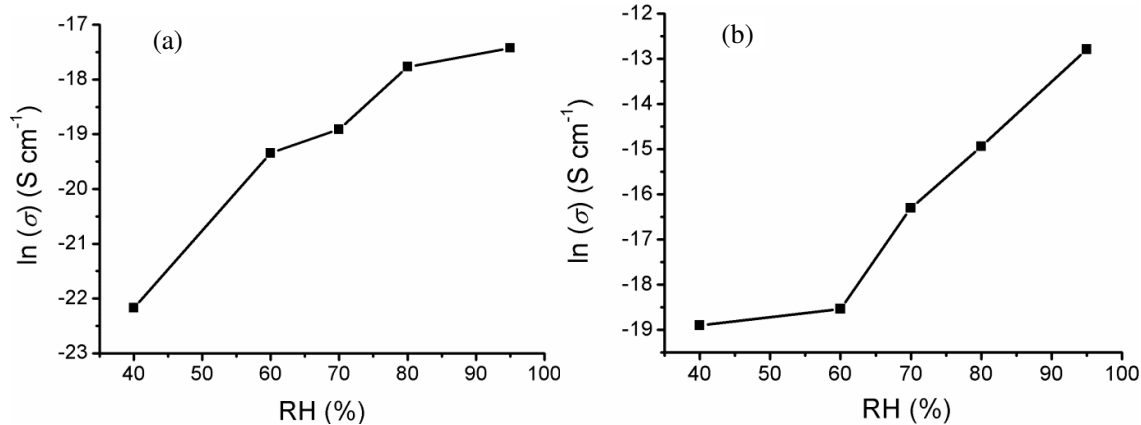


Fig. S15. Dependence of proton conductivity on relative humidity at 298 K for complexes **1** (a) and **2** (b).

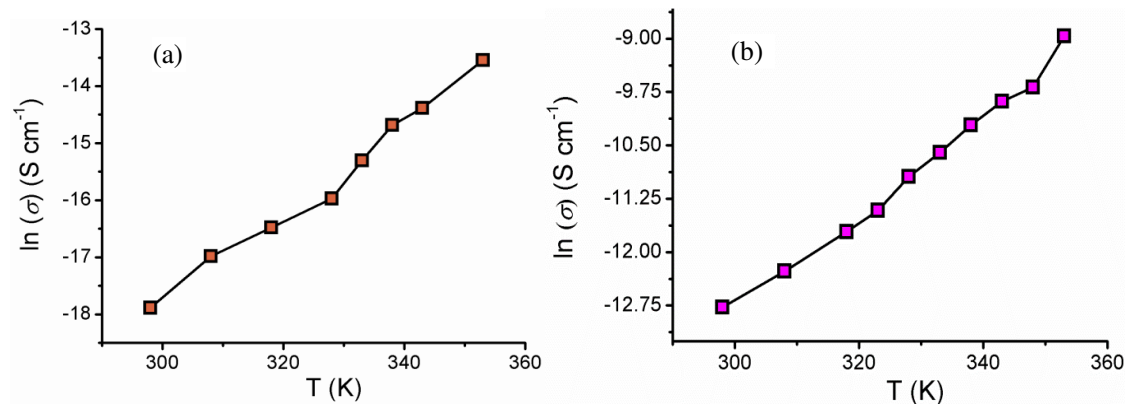


Fig. S16. Temperature dependency of proton conductivity at 95% relative humidity for **1** (a) and **2** (b).

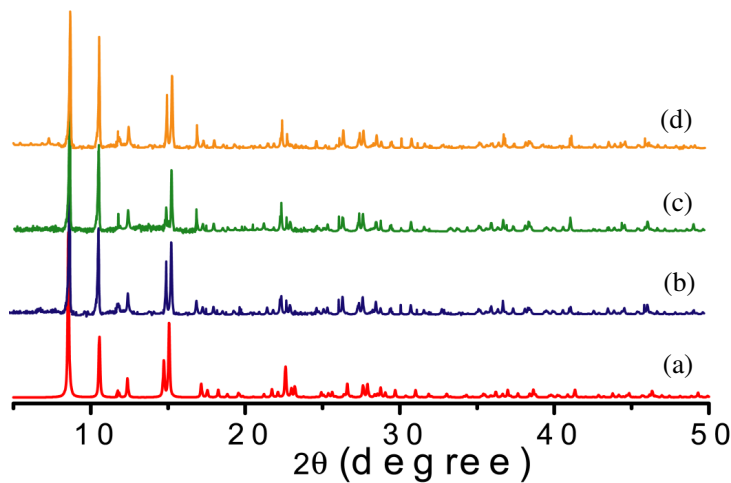


Fig. S17. Powder-XRD patterns for complex **1**. (a) simulated; (b) as-synthesized; (c) humidified (95% RH); (d) after impedance analysis.

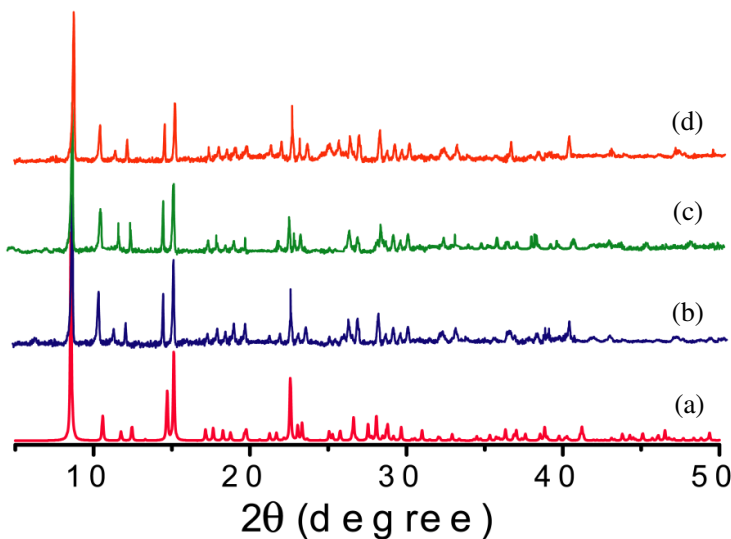


Fig. S18. Powder-XRD patterns for complex **2**. (a) simulated; (b) as-synthesized; (c) humidified (95 % RH); (d) after impedance analysis.

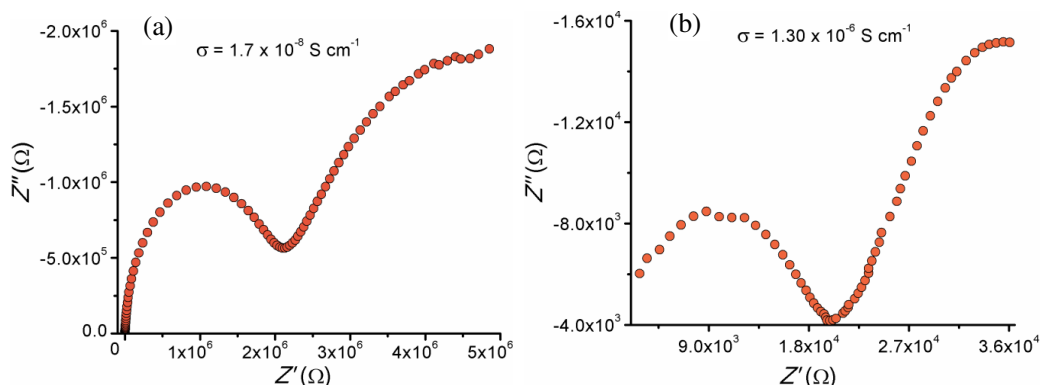


Fig. S19. Nyquist plots for proton conductivity of **1** at (a) 298 K and 95 % RH; (b) 353 K and 95 % RH.

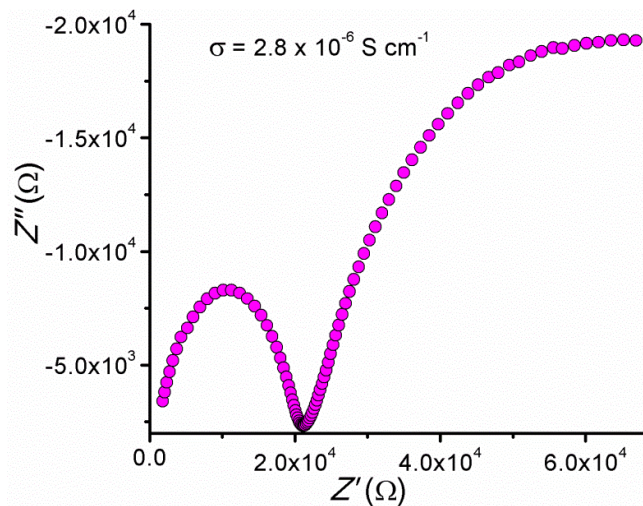


Fig. S20. Nyquist plot for proton conductivity of **2** at (a) 298 K and 95 % RH.

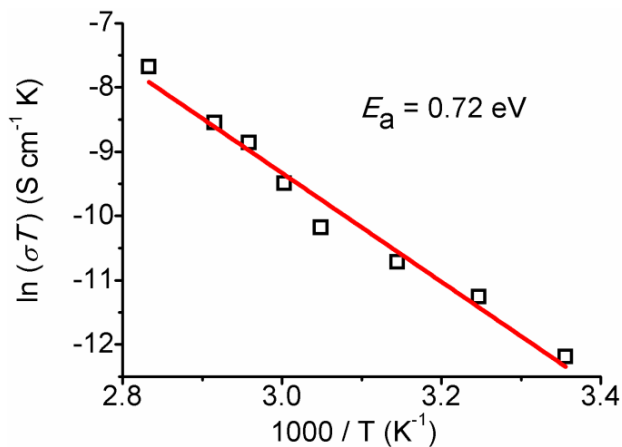


Fig. S21. Arrhenius plot for determination of activation energy (E_a) for **1**.

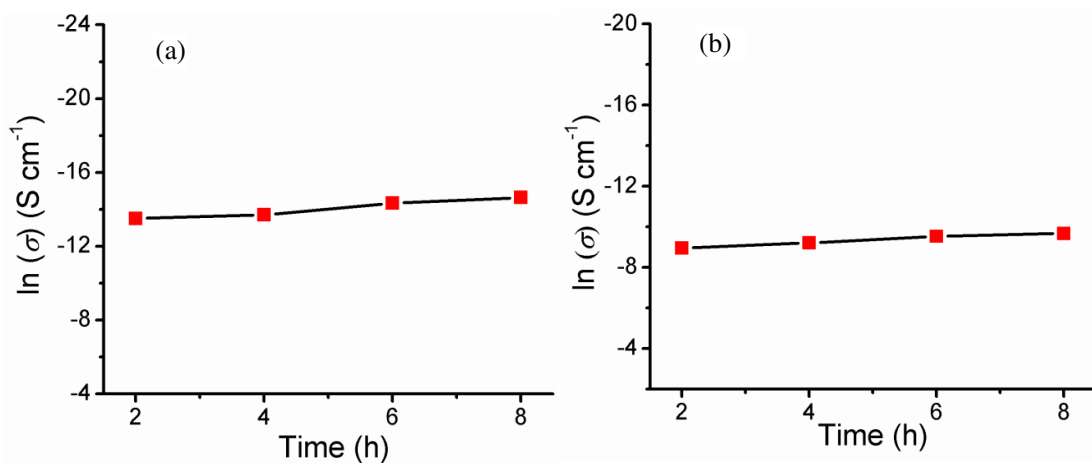


Fig. S22. Time-dependent proton conductivity of (a) complex **1** and (b) complex **2** at 80°C and 95% RH.

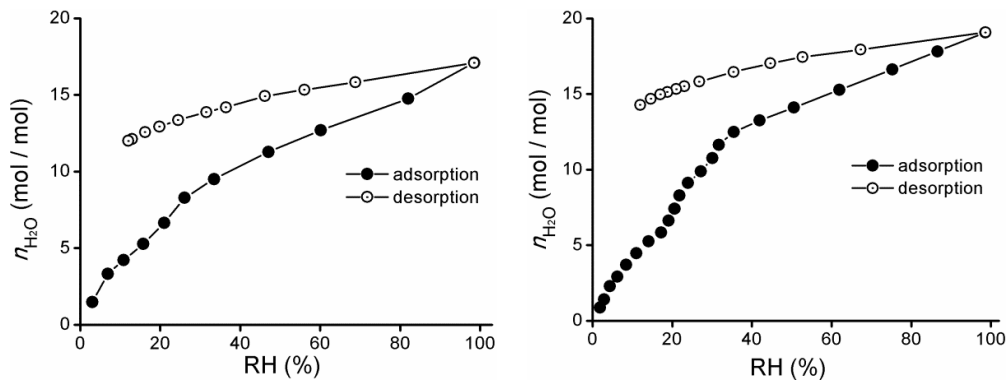


Fig. S23. Water vapor adsorption–desorption isotherms of complex **1** (a) and **2** (b).

Table S3. Some selected bond lengths (\AA) for complexes **1** and **2**.

1	Bond lengths (\AA)	2	Bond lengths (\AA)
Fe1—O15	2.099(5)	Co1—O7	2.067(4)
Fe1—O15A	2.099(5)	Co1—O7A	2.067(4)
Fe1—N2	2.153(3)	Co1—N1	2.101(3)
Fe1—N2A	2.153(3)	Co1—N1A	2.101(3)
Fe1—O3	2.154(3)	Co1—O6	2.121(3)
Fe1—O3A	2.154(3)	Co1—O6A	2.121(3)
Fe2—O4	2.121(3)	Co2—O3	2.082(3)
Fe2—O5	2.153(3)	Co2—O4	2.088(3)
Fe2—O11	2.098(4)	Co2—O5	2.113(3)
Fe2—O33	2.142(3)	Co2—O2	2.124(2)
Fe2—N3	2.188(3)	Co2—N2	2.124(3)
Fe2—N5	2.167(3)	Co2—N4	2.126(3)

Table S4. Some selected bond angles ($^\circ$) for complexes **1** and **2**.

1	Bond angles ($^\circ$)	2	Bond angles ($^\circ$)
O15A—Fe1—O15	89.4(4)	O7—Co1—O7A	88.3(4)
O15—Fe1—N2A	99.80(16)	O7—Co1—N1	96.99(14)
O15—Fe1—N2	91.67(16)	O7—Co1—N1A	91.91(14)
N2A—Fe1—N2	163.88(19)	N1—Co1—N1A	167.60(17)
O15A—Fe1—O3	88.4(2)	O7—Co1—O6	87.80(19)
O15—Fe1—O3	167.52(15)	O7A—Co1—O6	169.24(14)
N2—Fe1—O3	76.61(12)	N1—Co1—O6	78.62(10)
N2—Fe1—O3A	92.55(12)	N1A—Co1—O6	93.16(11)
O3—Fe1—O3A	96.32(19)	O6—Co1—O6A	97.73(17)
O11—Fe2—O4	166.30(13)	O3—Co2—O4	94.94(14)
O11—Fe2—O33	93.90(16)	O3—Co2—O5	169.60(12)
O4—Fe2—O33	88.67(14)	O4—Co2—O5	87.81(12)
O11—Fe2—O5	90.14(13)	O3—Co2—O2	88.49(13)
O4—Fe2—O5	103.28(12)	O4—Co2—O2	88.98(11)
O33—Fe2—O5	91.08(12)	O5—Co2—O2	101.60(11)
O11—Fe2—N5	89.51(14)	O3—Co2—N2	91.69(12)
O4—Fe2—N5	91.02(12)	O4—Co2—N2	90.41(11)
O33—Fe2—N5	166.81(13)	O5—Co2—N2	78.24(10)
O5—Fe2—N5	76.16(11)	O2—Co2—N2	179.38(10)
O11—Fe2—N3	89.48(13)	O3—Co2—N4	89.17(13)
O4—Fe2—N3	77.07(11)	O4—Co2—N4	165.86(12)
O33—Fe2—N3	89.52(13)	O5—Co2—N4	90.56(11)
O5—Fe2—N3	179.31(12)	O2—Co2—N4	77.58(10)
N5—Fe2—N3	103.27(12)	N2—Co2—N4	103.02(11)

Table S5. H-bond parameters found in complex 1.

D-H...A	D-H(Å)	H...A(Å)	D...A (Å)	\angle D-H-A(°)	Symmetry [#]
O11—H11A...O5	0.865	2.896	3.010 (5)	89.12	0
O11—H11B...O2	0.865	1.959	2.714(5)	145.14	0
O11—H11B...N3	0.865	2.789	3.018(5)	96.92	0
O15—H15B...O1	0.853	1.945	2.702(7)	147.31	0
O15—H15B...N2	0.853	2.795	3.051(7)	99.28	0
O33—H33A...O5	0.852	2.815	3.066(5)	98.96	0
O33—H33B...O4	0.852	2.734	2.979(5)	98.35	0
O11—H11A...O20	0.865	1.813	2.655(6)	163.95	1
O15—H15A...O15	0.853	2.776	2.953(9)	93.49	2
O15—H15A...O20	0.853	2.248	2.633(8)	107.47	3
O15—H15A...O23	0.853	2.747	3.473(6)	143.95	3
O33—H33A...O1	0.852	2.592	3.163(6)	125.35	4
O15—H15A...O23	0.853	2.747	3.473(6)	143.95	4
O33—H33B...O1	0.852	2.968	3.163(6)	95.30	4
O15—H15A...O23	0.853	2.747	3.473(6)	143.95	5
O15—H15A...O23	0.853	2.747	3.473(6)	143.95	6
O33—H33B...O3	0.852	2.036	2.841(5)	157.26	6
O15—H15B...O21	0.853	2.984	3.606(2)	131.54	7
N1—H1...O7	0.860	2.003	2.852(5)	168.92	7
O33—H33A...O22	0.852	2.067	2.753(2)	137.18	8
N4—H4...O5	0.860	2.261	3.040(5)	150.62	9
N4—H4...O5	0.860	2.261	3.040(5)	150.62	10

(0) x,y,z; (1) -y+1,+x+1/2,+z-1/2; (2) -x+1/2,-y+1/2,+z; (3) x,+y,+z-1 (4) y,-x+1/2,-z+1/2; (5) -x+1/2,-y+1/2,+z-1 (6) -y+1/2,+x,-z+1/2;
 (7) -x+1,-y+1,-z; (8) -y+1,+x-1/2,+z+1/2; (9) -y+1,+x-1/2,+z-1/2; (10) y+1/2,-x+1,+z-1/2.

Table S6. H-bond parameters found in complex 2.

D-H...A	D-H(Å)	H...A(Å)	D...A (Å)	\angle D-H-A(°)	Symmetry [#]
O3—H3A...O2	0.884	2.779	2.934(4)	91.27	0
O3—H3B...O8	0.882	2.018	2.710(5)	134.44	0
O3—H3B...N2	0.882	2.859	3.018(4)	91.72	0
O4—H4A...O5	0.918	2.831	2.913(4)	85.92	0
O4—H4A...N2	0.918	2.902	2.989(4)	86.42	0
O4—H4B...O3	0.919	2.914	3.073(5)	91.12	0
O3—H3A...O11	0.884	1.804	2.664(6)	163.89	1
O4—H4A...O6	0.918	1.926	2.839(4)	172.94	2
O4—H4B...O12	0.919	2.881	3.650(2)	142.16	3
O4—H4B...O13	0.919	2.420	2.794(2)	104.38	4
O4—H4B...O13	0.919	2.477	3.242(2)	140.95	5
N3—H3...O1	0.860	2.012	2.862(4)	169.33	5
O7—H7A...N1	1.002	2.900	2.997(6)	85.72	6
O7—H7A...O9	1.002	1.885	2.690(6)	135.18	6
O7—H7B...O11	0.998	1.868	2.648(7)	132.67	7
N5—H5...O2	0.860	2.285	3.065(5)	150.84	8
N5—H5...O2	0.860	2.285	3.065(5)	150.84	9

(0) x,y,z; (1) y+1/2,-x+1,+z+1/2; (2) -y+1/2+1,+x+1,-z+1/2+1; (3) y+1/2,-x+2,+z+1/2; (4) x,+y,+z+1; (5) -x+1,-y+2,-z+1; (6) -x+1/2,-y+1/2+2,+z; (7) x,+y+1,+z; (8) -y+1,+x+1/2,+z-1/2; (9) y-1/2,-x+1,+z-1/2.

References

1. O. Kahn, *Molecular Magnetism*, VCH publishers, New York, 1993.
2. G. Sheldrick, *SHELXL-97, Program for Crystal Structure Refinement*; University of Gottingen: Gottingen, Germany, 1997.